Coastal Engineering Journal

Nationwide Post Event Survey and Analysis of the 2011 Tohoku Earthquake Tsunami

NOBUHITO MORI
Disaster Prevention Research Institute, Kyoto University, Kyoto 611-0011, Japan.
mori@oceanwave.jp

TOMOYUKI TAKAHASHI
Faculty of Safety Science, Kansai University, Takatsuki, Osaka 569-1098, Japan.
tomot@kansai-u.ac.jp

THE 2011 TOHOKU EARTHQUAKE TSUNAMI JOINT SURVEY GROUP
http://www.coastal.jp/tsunami2011/
dpri@oceanwave.jp

Received (3 October 2011)
Revised (13 January 2012)

At 14:46 local time on March 11, 2011, a magnitude 9.0 earthquake occurred off the coast of northeast Japan. This earthquake generated a tsunami that struck Japan as well as various locations around the Pacific Ocean. With the participation of about 300 researchers from throughout Japan, joint research groups conducted a tsunami survey along a 2,000 km stretch of the Japanese coast. More than 5,200 locations have been surveyed to date, generating the largest tsunami survey dataset in the world. The inundation height and run-up height were surveyed by laser, GPS and other instruments, and the tidal correction has been accurately adjusted using a tidal database and a numerical simulation for Tohoku, an area where tide gauges were destroyed by the tsunami. Based on the survey dataset, the regional and local scale analyses were conducted to understand the basic characteristics of this event. Maximum run-up heights greater than 10 m are distributed along 500 km of coast in direct distance. The affected area of this event was several times larger than historically recorded in Tohoku. The mean inundation height in the southern Sanriku region is 10-15 meters and there are several peaks of inundation along the coast from the northern to middle part of Sanriku.

Keywords: Tsunami; post event survey; inundation height; run-up height

1. Introduction

The 2011 Tohoku Earthquake Tsunami was a tremendous and tragic earthquake-tsunami disaster for Japan. An earthquake of magnitude 9.0 occurred off the Pacific coast of Tohoku, Japan, on March 11, 2011, at 14:46:23 Japan Standard Time (+9

UTC). The rupture area, assumed to be approximately 450 km × 200 km, generated a tsunami 130 km off the coast of Miyagi Prefecture, in northeast Japan. This tsunami is the fourth mega earthquake-generated tsunami occurring this century [*e.g.* Largest Earthquakes in the World Since 1900, 2011]; the other three were the the 1960 Chile Earthquake Tsunami, the 1964 Alaska Earthquake Tsunami and the 2004 Sumatra Earthquake Tsunami [Liu et al., 2005; Fujima et al., 2006; Matsutomi et al., 2006]. Another large earthquake tsunami also occurred in Chile last year [Michelini et al., 2010].

Three minutes after the start of the Tohoku Earthquake, tsunami warnings were issued by the Japan Meteorological Agency. The tsunami first reached the Japanese mainland 20 min after the earthquake and ultimately affected a 2,000 km stretch of Japan's Pacific coast [Mori et al., 2011]. The Tohoku region comprises several prefectures ranging from north to south: Aomori Prefecture, Iwate Prefecture, Miyagi Prefecture, and Fukushima Prefecture, which border the Pacific Ocean. Sendai is the largest city in the region. The southern part of Tohoku is relatively flat, especially the Sendai Plain, but the coastal geomorphology of northern Tohoku features ria coasts, which are steep, narrow bays. The northeastern part of Tohoku is known as the Sanriku region. The tsunami inundated over 400 km^2 of land. As of January 13 in 2012, official fatalities were 15,844 with an additional 3,394 missing. The major cause of death was the tsunami, and most fatalities occurred in Tohoku: 58% in Miyagi Prefecture, 33% in Iwate Prefecture and 9% in Fukushima Prefecture, respectively. The number of totally and partially damaged houses, buildings and bridges were 128,530, 230,332 and 78, respectively.

Before this event, the risk of an earthquake and tsunami off the Tohoku coast was believed to be high. The Japanese government reported that a magnitude 7.4 earthquake along a 200 km fault offshore of Sendai was expected to occur with 99% probability within 30 years. The 1896 Meiji Sanriku earthquake (Mw 8.2-8.5) and tsunami caused 21,915 deaths, the 1933 Showa Sanriku earthquake (Mw 8.1) and tsunami caused 3,064 deaths, and smaller tsunamis have occurred roughly every 10 to 50 years. Thus, earthquake and tsunami disaster countermeasures, such as offshore and onshore tsunami barriers, planted trees as a natural tsunami barrier, vertical evacuation buildings, and periodic evacuation training were implemented and practiced in these areas. Therefore, we emphasize that Tohoku was an area highly prepared for a tsunami. Nevertheless, the tsunami disaster countermeasures were insufficient against the 2011 event. Tsunami barriers were severely damaged, some reinforced concrete buildings were totally destroyed, and the extent of inundation was underestimated in several areas.

Numerical simulation is the most important tool to help prepare for future tsunamis. There are several uncertainties associated with tsunami projections in earthquake prone locations. The first component to be considered is assuming an initial tsunami profile at the source. The initial tsunami profile is a major research topic in tsunami research, and it depends on the sea bottom slide, although the state of

art of seismology study was insufficient at projecting the 2011 Tohoku Earthquake Tsunami beforehand. This is a key topic in tsunami research, and it is not limited to tsunami researchers. Offshore tsunami simulation technology has greatly improved in the last few decades [*e.g.* Goto and Ogawa, 1991; Ioualalen et al., 2007]. Both estimation of maximum tsunami height and its arrival time are important for tsunami forecasts Kumar et al. [2006], the inversion of tsunami profile is necessary to be improved [Lay et al., 2011]. If an initial tsunami profile is correctly given, the propagation of a tsunami to the shoreline can be computed by nonlinear or linear long wave equations accurately. Once the tsunami reaches the shoreline, tsunami inundation modeling becomes difficult and complicated. Local tsunami characteristics are sensitive to high resolution bathymetric data, wave breaking, and diffraction, or processes described with the standard shallow water equation. The characteristics are also related to bore formation, debris, other hydrodynamic effects, locations of buildings, streets, and other elements of urban topographic effects [*e.g.* Karlsson et al., 2009]. The latter components are related to both wave dynamics and fluid dynamics, and they are not well understood or modeled yet, although it is important to estimate the damage to structures [*e.g.* Tomita et al., 2006; Yamamoto et al., 2006]. Therefore, real field data are necessary to understand and model these phenomena, but these data are limited because extreme tsunami events are very rare given the return periods. In addition, academic knowledge aside, organizing a large survey group and collecting copious amounts of field data with people of varying backgrounds of field and survey experience was challenging, and many difficulties were encountered.

This paper summarizes the results of a post-event field survey of the 2011 Tohoku Earthquake Tsunami and documents how we conducted the survey and summarized the data. First, an overview of the survey is presented, and the organizing survey group and data-collecting procedures are summarized. Second, the process of compiling the tsunami survey data set and validating the systematic tidal correction are presented. Third, the tsunami inundation heights and run-up heights are discussed for a regional and bay scale analysis. Finally, the accuracy behind estimating maximum tsunami height and arrival time by numerical model is discussed for future tsunami warning systems.

2. Method

2.1. *Overview of Survey*

Tsunami surveys were conducted by joint research groups with the participation of 299 tsunami, coastal, seismology and geology researchers from 64 universities and institutes throughout Japan [The 2011 Tohoku Earthquake Tsunami Joint Survey Group, 2011]. A discussion about organizing a survey group began soon after the earthquake via a tsunami research e-mail list and web site, which was newly reformed after the original server hosted by Tohoku University had been damaged

from the earthquake and related power outages since March 11. The 2011 Tohoku Earthquake Tsunami Joint Survey Group (hereinafter, the survey group) is autonomous survey organization and it consists of members from different fields of natural science, tsunami engineering, coastal engineering, and tsunami-related research; the survey group was managed with researchers at the Faculty of Safety Science of Kansai University and the Disaster Prevention Research Institute of Kyoto University (denoted survey secretariat), because these two universities have available staff and are located in western Japan, an area that was largely unaffected by the earthquake.

Surveys began within two days after the earthquake in less severely affected areas (Ibaraki Prefecture, Chiba Prefecture, and other prefectures outside Tohoku), and surveys in Tohoku began March 25 after the completion of major search and rescue operations in severely affected areas. Until the middle of April, teams were assigned to survey locations by the survey secretariat to ensure survey efficiency and to avoid interfering with relief operations. Preliminary measurement results, aerial and satellite images, and eyewitness accounts were used for initial guidance in selecting survey areas given the lack of information on road and bridge conditions and the limited availability of food and gasoline. Although the survey areas were wide, the local situations and survey conditions were very severe initially. Only thirteen expert survey teams conducted surveys in Tohoku from March 25 to April 8, and thereafter general survey teams including novice members conducted surveys. The survey areas were gradually expanded to all of the Tohoku region after the middle of April. Survey groups measured local tsunami heights along the coast stretching 2,000 km from Hokkaido in the north to Okinawa in the south, with the exception of a 30 km zone around the Fukushima Daiichi Nuclear Power Plant [Watanabe et al., 2012; Ogasawara et al., 2012; Shimozono et al., 2012; Suppasri et al., 2012; Gokon and Koshimura, 2012; Kakinuma et al., 2012; Suppasri et al., 2012; Udo et al., 2012; Tanaka et al., 2012; Mikami et al., 2012; Sasaki et al., 2012].

The height of a tsunami can be defined in three ways: 1) the tsunami height, or the height of the wave until it reaches the shoreline; 2) the maximum water level (hereinafter, inundation height); and 3) the run-up height. These three heights are measured from sea level, generally excluding the astronomical tide [Intergovernmental Oceanographic Commission; IOC-UNESCO, 1998]. Inundation and run-up were measured within a few centimeters accuracy from watermarks on buildings, trees, and walls using laser range finders, a real-time kinematic (RTK) GPS receiver with cellular transmitter, and total stations. Run-up height was determined from the maximum landward extent of debris and seawater marks.

The measurement data were sent to the survey secretariat and immediately converted into Google Keyhole Markup Language and made available on the Joint Survey Group web site (see Figure 1). This procedure was important to prevent different survey teams from collecting measurements at an already surveyed location. The survey group mailing list was used to plan survey activities and to keep teams informed of the latest conditions in the survey areas. In this way, the activities of

the different teams could be coordinated and the survey area could be expanded and managed efficiently. As of the end of December 2011, the total number of survey locations was 5,214.

2.2. *Inundation and Run-up Heights Dataset*

Mainly two different measurement methods were conducted for the local tsunami height survey. One method involves relative measurements from the sea surface to a watermark, and the other requires elevation (altitude) measurements from a triangulation point to a watermark. The tidal correction for relative measurements requires tidal elevations for both maximum tsunami arrival time and survey time, and elevation measurements require tidal elevations at the tsunami arrival time. The survey data were corrected for tidal elevations at the time of maximum tsunami height following the IOC-UNESCO guideline [Intergovernmental Oceanographic Commission; IOC-UNESCO, 1998] as shown in Figure 2. The tidal correction was conducted using far field data from tide gauges and an astronomical tidal database for the near field locations as shown in Figure 2. Due to physical damage to tide gauges along the Tohoku coast of Japan, the astronomical tidal database maintained by the National Astronomical Observatory of Japan, NAOTIDEJ, was used for tidal correction from Aomori to Ibaraki Prefectures (near field). The reason for using the tide gauge data for far field correction will be explained later. The tsunami arrival time was estimated by numerical simulation for the near field and was determined by tidal gauge measurements in other areas.

Data on inundation distances were primarily determined by survey measurements. Unmeasured inundation distances were estimated with the World Vector Shoreline dataset from the U.S. National Geospatial-Intelligence Agency. The minimum distance from the shoreline, excluding lakes and rivers, was taken as the inundation distance.

A numerical simulation was conducted to estimate the arrival time of the largest tsunami wave by using the nonlinear long-wave equation with spherical coordinates. The main purpose of this numerical simulation is to estimate the arrival time of the maximum tsunami height. The governing equation is discretized with the explicit leap-frog finite difference scheme. In the spatial domain, all of Japan is covered at a resolution of 0.5 minutes by JTOPO30 bathymetry data (30 second resolution). Three different initial tsunami profiles were used in the tsunami simulations. Two forty-subfault models (version 4.2 and 4.6; denotes FS40v42 and FS40v46 hereafter) and one-subfault model (FS1) by Fujii et al. [2011] and the two-subfault model (GSI2) by the Geospatial Information Authority of Japan (GSI) [2011] were used and validated with the measurement data. The forty-subfault models (FS40v42 and FS40v46) and one-subfault model (FS1) by Fujii et al. [2011] gave one of accurate comparison against observed data; thus, the results using the FS40v46 were used for tidal correction. In addition, the numerical results using three different initial conditions provide interesting results in terms of the accuracy of the tsunami simu-

lation, which will be discussed later. Using numerical results and an astronomical tidal database, the astronomical tidal levels were estimated from Aomori Prefecture to Ibaraki Prefecture, where most of the tide gauges were destroyed by the tsunami.

2.3. *Numerical Accuracy of Tsunami Arrival Time Estimate*

To validate the tsunami arrival time by numerical simulation, the nonlinear long-wave solution was compared with the tsunami heights measured by tide gauges along the shoreline; the results proved interesting differences against tide gauge data. Figure 3 shows the differences in maximum tsunami height and arrival time between the numerical results and measurement data collected by JMA tide gauges. As mentioned in the previous section, three initial tsunami profiles from different inversion methods were considered for the computations. As shown in Figure 3, the absolute accuracy of the maximum tsunami height basically depends on the distance from the epicenter. The tide gauge at Onahama Port in Fukushima Prefecture was the tide gauge closest to the epicenter that remained operable; the data from this gauge indicate that the error associated with the maximum tsunami height of 6.3 m depends on the fault model. The maximum error monotonically decreases with increasing distance from the epicenter. The mean error values for maximum tsunami height are 0.6 m, 0.7 m, and 0.6 m in the FS40v46, FS1, and GSI2 models, respectively. The relative error in maximum height becomes larger because far from the epicenter the tsunami height itself is also small. Estimating the arrival time of the maximum tsunami height provides important information for evacuation plans. Figure 3 shows the relative error of the arrival time of the maximum height from the numerical models. In contrast to the maximum tsunami height, the error of the arrival time monotonically increases with increasing distance from the epicenter. The mean errors associated with the maximum tsunami arrival times are 1.8 hr, 2.2 hr and 2.1 hr for the FS40v46, FS1, and GSI2 models, respectively. The error of maximum tsunami arrival time is more than 3 h at a distance of approximately 400 km from the epicenter, and the numerical model basically gives arrival times that are slower than observed data. In estimating tsunami arrival time, the difference between the initial tsunami profiles is less important than the distance from the epicenter, although FS40v46 gives the best results of the three initial profiles. Therefore, the difference arises from the numerical scheme itself rather than from different initial configurations.

To summarize this section: for the tidal correction, we will use the results of FS40v46 to estimate the arrival time of the maximum tsunami height for the near field, from Aomori Prefecture to Ibaraki Prefecture.

2.4. *Validation of Tidal Correction*

Tidal correction was conducted by using data from an astronomical tidal database for the near field as mentioned above. The astronomical tidal database of the

National Astronomical Observatory of Japan, NAOTIDEJ, was used for the tidal correction; it is a numerical astronomical tidal database relative to MSL with 10 km resolution for the entire country of Japan. Therefore, the database provides better spatial resolution to estimate astronomical tides if the accuracy of the database is satisfactory and reasonable.

The validation of the database against observed tidal elevations at Hachinohe, Ofunato and Sendai in Tohoku, is shown in Figure 4. The solid lines in the figure indicate tidal elevations from the database, and the dashed lines indicate observed tidal elevations measured by tidal gauge. The mean absolute differences and mean standard differences between the two tidal elevations are 6.0 cm and 7.7 cm, respectively. The accuracy of the NAOTIDEJ database is reasonable to use for tidal estimates in the near field.

Figure 5 shows the validation of the total tidal correction for relative tsunami height measurements. The upper panel illustrates the correlation of the total tidal elevation (the tidal elevation at survey time minus the tidal elevation at maximum tsunami arrival time) between the nearest tide gauge and the database for survived tide gauges in Tohoku. The correlation between these variables is 0.7, indicating reasonable accuracy although there are some scatter points. The lower panel illustrates the histogram of relative error of total tidal elevation between the nearest tidal gauge and the database for the survived tide gauges in Tohoku. The averaged absolute difference is 17.3 cm and the standard deviation is 25.0 cm, respectively. Error is also inherent with estimating tidal elevations from gauges, thus the tidal correction by database for the near field gives quite reasonable results over the entire Tohoku area with a 10 km spatial resolution. Using the systematically collected data and tidal correction, the large dataset of tsunami inundation and run-up heights was summarized by the secretariats of joint survey group.

3. Distribution of Tsunami Heights

The offshore and onshore tsunami heights were measured by NOAA's DART buoys in the Pacific Ocean, NOWPHAS GPS buoys operated by the Port and Airport Research Institute of Japan, and tide gauges operated by Japan Meteorological Agency on the shoreline. The NOWPHAS GPS buoys were located 2 km offshore and a few buoys measured tsunami heights of 8.0-8.5 m off the coast of Iwate Prefecture about 30 min after the earthquake. Buoy-measured tsunami data have been summarized by several agencies [*e.g.*, the Japan Weather Association [http://www.jwa.or.jp/static/topics/20110329/touhokujishin110329.pdf]]. Here, we focus on data about the tsunami after it reached land.

Temporal and spatial differences were evident. In Miyagi Prefecture, closest to the epicenter, the first wave was the largest. In Chiba Prefecture to the south, the third wave, arriving three hours after the first, was the largest. This tsunami was remarkable not only for the magnitude of the event, but also for the wide variety of inundation characteristics – from urban cities with modern coastal defenses to

rural coastal towns and agricultural lands. Local coastal geomorphology also differed substantially across the affected region; for example, the urban center of Sendai (population 1 million) is situated on a fluvial lowland, and smaller cities and towns to the north are situated on a ria coast with steep terrain.

Figure 6 shows an overview of inundation heights and run-up heights in Japan and on the Sendai Plain. Effects of local coastal geometries can also be readily seen. The local geomorphology of Sendai City and its suburban areas feature a fluvial lowland and flat coastal plain, and the tsunami bore propagated inland. From about 50 to 200 km north of the Sendai Plain, the local geomorphology of the Sanriku region is characterized by ria coast, steep terrain, and shallow, narrow bays; these features focused the tsunami waves, generating the largest run-ups and resulting in the catastrophic destruction of towns and cities including Taro, Miyako, and Rikuzen-Takata in Iwate Prefecture.

As shown in Figure 6, the inundation heights and run-up heights are high from Tokyo to Hokkaido, and are separated by a distance that corresponds to approximately two times the distance between Banda Aceh and Phuket Island. Local topography amplified the tsunami height in many bays, and this amplification due to trapped edge waves was also observed along plane beaches. The maximum inundation height in Hokkaido was 6.78 m along plane beaches. The maximum inundation heights in the Tokyo Bay area, Shikoku, and Kyushu were 2.8 m, 3.3 m, and 1.0 m, respectively. Tokyo Bay, Shikoku, and Kyushu are located about 390 km, 1,000 km, and 1,300 km to the southwest of the epicenter as measured directly. These maximum inundation heights were observed in bays where the local geometry amplified the tsunami wave at the end of the bay [*e.g.*, [Sasaki et al., 2012]].

The Sendai Plain is the most populous area in Tohoku and consists of a fluvial lowland and a flat coastal plain formed by the Abukuma, Natori, and Nanakita Rivers. The dynamics profile changes of beach and river delta were observed along the coast [Udo et al., 2012; Tanaka et al., 2012]. A high spatial density of inundation heights was measured at more than 1,000 locations on this plain (Figure 7). The maximum inundation height was 19.50 m, and the mean inundation height near the shoreline was about 10 m. As can be seen in the figure, the tsunami bore propagated inland, deeply. The monotonical decrease in inundation height from the shoreline inland can be seen, but local geometric effects such as rivers also produce significant effects. The regional analysis will be discussed in Section 4.

The eastern coast of Tohoku runs in the north-south direction along the Pacific Ocean. Figure 8 shows the projected inundation heights and run-up heights along the latitudinal direction with historical tsunami records from the 1896 Meiji Sanriku Tsunami (Mw 8.2-8.5) and 1933 Showa Sanriku Tsunami (Mw 8.4), respectively. In the 2011 Tohoku Tsunami, the maximum run-up height was 40.0 m at Ofunato, which resulted in catastrophic destruction of towns and cities in the ria coast area (lat 38-40°N). The historical records of maximum run-up are 38.2 m for the 1896 Meiji Sanriku Tsunami and 28.7 m for the 1933 Showa Sanriku Tsunami (Figure 8).

The maximum run-up height for the 2011 event is similar to that for the Meiji Sanriku Tsunami, but the stretch of affected coastline is several times larger for the Tohoku Tsunami than for the Meiji Sanriku Tsunami. The areas where the maximum run-up height exceeded 30 m extend from Onagawa to Noda, which covers more than 180 km of the Sanriku coast. Maximum run-up heights greater than 10 m are distributed along 530 km of coast, and maximum run-up heights greater than 20 m are distributed along 200 km of coast, as measured in direct distances.

The size of the 2011 Tohoku Tsunami was much larger than expected; given the uncertainty behind tsunami generation, tsunami modeling using historical records did not predict this tsunami well. On the other hand, the vertical and horizontal distributions of run-up height are similar and more intense for the 2011 Tohoku Tsunami than for the 2004 Indian Ocean Tsunami [*e.g.* Karlsson et al., 2009]. The gap in data located about lat 37.5°N in Figure 8 is the 30 km restricted area around the Fukushima Daiichi nuclear power plant. The maximum run-up heights located 30 and 40 km from the nuclear power plant were 16.9 m and 21.3 m, respectively. The run-up heights near the south of Fukushima Daiichi were higher than in the middle of the Sendai Plain, even though Fukushima Daiichi is farther from the epicenter. Compared with the northern Sendai Plain, the southern Sendai Plain has a steeper and narrower continental shelf, which amplified the tsunami height and caused severe damage to the Fukushima Daiichi plant.

4. Regional and Locational Distributions of Inundation Height and Run-up Height

The behavior of the tsunami on land shows a clear regional dependence. Figure 9 shows the inundation heights and run-up heights in seven areas as a function of distance from the shore line. The panels in Figure 9 show data for (A) Hokkaido, (B) Iwate Prefecture, (C) North Miyagi Prefecture, (D) South Miyagi Prefecture, the Sendai Plain, (E) Fukushima Prefecture, (F) Ibaraki Prefecture, and (G) Chiba Prefecture and Tokyo. The lines in the figure indicate exponential decay with increasing distance from the shoreline. At locations far from the epicenter (Figure 9(A) and (E)-(G)), inundation occurred within 1 km of the shoreline, except at several locations near a river. On the other hand, inundation extended farther inland on the Sendai Plain (Figure 9(D)). Run-up decayed exponentially with increasing distance, up to 5 km inland from the shoreline; however, much longer tsunami run-ups were measured along rivers [Suppasri et al., 2012; Gokon and Koshimura, 2012]. The inundation height in Sanriku (Figure 9(B) and (C)) is two times higher than that on the Sendai Plain, but inundation did not extend as far inland in Sanriku. The tsunami energy was converted to run-up height rather than to inundation distance for these areas [Kakinuma et al., 2012]. In southern Sanriku (Figure 9(C)), however, there are several rivers and small fan deltas such as Rikuzen-Takata and Minami-Sanriku; long run-ups following the rivers were measured in these areas. On average, the characteristic of inundation height decreasing with increasing distance

from the shoreline is different between Sanriku and the Sendai Plain. Accordingly, detailed analysis is needed at the regional level.

A major difference between the 2011 Tohoku Earthquake and Tsunami and the 2004 Indian Ocean Tsunami is the extent that the local areas in Japan were prepared for tsunami inundation and mitigation measures. Before the 2011 event, the likelihood of an earthquake inducing a tsunami off the coast of Japan was considered to be high. Buildings in the Sanriku area were designed and built to resist earthquakes, and both hard structural and natural tsunami barriers were constructed and implemented. Despite the planning and preparedness, tsunami barriers were severely damaged, some reinforced concrete buildings were totally destroyed, and inundation occurred beyond the boundaries depicted on inundation maps for several areas. For future planning, a high-density database of inundation and run-up information can be analyzed to assess local tsunami behavior in the inundated areas.

For example, Figure 10 shows local analysis of inundation height and run-up height at Otsuchi Bay and Kamaishi Bay in Iwate Prefecture. The distance between the two bays is about 10 km, and they have similar water depths of about 50-55 m at the bay mouths. Before the 2011 event, both bays had similar historical run-up records and expected tsunami heights. The maximum run-up heights at Otsuchi Bay and Kamaishi Bay in the 1896 Meiji Sanriku Tsunami were 6.0 m and 8.0 m, respectively. However, an offshore tsunami barrier was installed in Kamaishi Bay in 2009; this barrier is located 2.2 km from the bay mouth and 2.3 km from defined shoreline in Figure 10 (b). The measurement data on inundation height and run-up height will be useful to investigate the effectiveness of tsunami protection for this event.

The three lines in the lower panel of Figure 10 indicate changes in inundation height and run-up height, according to Green's law, from the bay mouth to the shoreline considering only water depth change (dashed line), only bay width change (dash-dotted line) and both water depth and bay width changes (solid line). The water depth change and bay width change are simply assumed to be linear from the bay mouth to the shoreline. The starting height of the theoretical curves at the bay mouth is arbitrary in this analysis; therefore, the curve indicates only qualitative amplification of tsunami heights from offshore to onshore. Open box and open triangles in the upper right panel of Figure 10 respectively indicate locations of the bay mouth and the most distant shoreline from the bay mouth, and the solid vertical line in the lower panel indicates the shoreline. We selected measured inundation and run-up heights along the coast line of the ria coast. Although these are land side measured data, they can also be regarded as near coastal data. In Otsuchi Bay the run-up height is initially 17 m at the bay mouth and maintains a height of 15-19 m to the shoreline, whereas in Kamaishi Bay the run-up height is initially 22 m at the bay mouth, drops to 10 m near the offshore barrier, and remains roughly constant at 10 m up to the shoreline. The theoretical curve from Green's law considers bay width changes and agrees well with the upper limit of

measurement data. The reduction in tsunami height is mainly due to the absence of detailed local bathymetry in the numerical runs, but the Green's law basically provides a good indication of the possible upper limit for each bay. The differences in tsunami protection between these two geometrically similar bays can be seen in this Figure. This database should help verify the effectiveness of hard structure tsunami barriers. Furthermore, a notable feature of the data is that local inundation heights and run-up heights differed between neighboring locations a short distance from each other. Sea walls, complex shading and diffraction by structures, and debris may play important roles in changing local tsunami behavior. These influences lead to local changes in inundation and run-up heights, causing them to differ from historical records. These macro roughness effects in the inundation areas are also difficult to consider numerically using the standard long-wave equation. Our survey results will be made available as a standard dataset for validating numerical code.

As indicated in Figure 10, local bathymetry and other effects are significant. To understand the local effects on tsunami inundation behavior, the bay scale analysis was conducted using the survey data and topographical and bathymetric bay information. Figure 11 shows the mean inundation height at individual ria coast bays from Aomori Prefecture to Miyagi Prefecture. Ignoring the spatial density of the measurements points, simple spatial averaging was applied for each bay. Apart from Onagawa in the southern part of Sanriku, the mean inundation height in southern Sanriku is 10-15 meters. Interestingly, the mean inundation height is large in the middle part of Sanriku between Rikuzen-Takata and Funakoshi Bays (39.00-39.50°N) rather than other areas. There are other large peaks of mean inundation height in the northern part of Sanriku, from Taro to Noda villages (39.75-40.10°N) where this tsunami wreaked severe damages Ogasawara et al. [2012].

On the other hand, the simulated maximum tsunami heights show slightly different distributions for the northern coast of Sanriku. Figure 12 shows the results of four of simulations using the differnt subfault models as an initial condition described previously. The simulated maximum tsunami height is basically large in the southern part of Sanriku and monotonically decreases as the latitude increases. The most of numerical results reasonably agree with the southern part of Sanriku (lower than 39.0°N) and Aomori Prefecture (higher than 40.5°N). The local comparisons between the survey and numerical results have been coducted by other people (*e.g.*, Hokkaido area by Watanabe et al. [2012], Middle and South of Sanriku by Shimozono et al. [2012]; Kakinuma et al. [2012], Tokyo area by Sasaki et al. [2012]) show qualitatively agree with our results. There are no significant differences between the other initial tsunami profiles, such as FS1, GSI2 or others above 39.0°N around the northern part of Sanriku to Aomori Prefecutre. However, there are no clear increases in the simulated maximum tsunami heights above 39.0°N around the northern part of Sanriku, or the area from Taro to Noda villages where the survey data show clear increases in the mean inundation heights as indicated in Figure 11. All of simulated results are different from the survey data, if the differences between

simulated tsunami heights and measured inundation heights are neglected. Additionally, the initial faults that were estimated may not have considered slower ground motion north of the epicenter [*e.g.* Lay et al., 2011; Koketsu et al., 2011]. Further investigation will be required to understand from the source to land for this event.

The inundation height (or local tsunami height) measured on land is different from the simulated maximum tsunami height at the shoreline. However, a tsunami height at the shoreline is a boundary condition for inundation modeling and therefore the parameters should be highly related to each other. For instance, it is assumed that the tsunami amplification factor simply follows a linear relation.

$$H(x) = ax + b \tag{1}$$

where x is the spatial coordinate in kilometers, beginning from the bay mouth to the inner bay, $H(x)$ is inundation height in meters perpendicular to the x direction, and a and b are empirical coefficients, respectively. The coefficients a and b are estimated from survey data considering the bay profile using the least squares method. The local tsunami amplification factor generally follows Green's law as discussed previously. Therefore, the local tsunami height, $H(x) \propto x^n$, depends on changes in water depth and bay width or the bathymetry and topography of each bay. However, empirical fitting for the power law of the coefficient n is sensitive to the data and fitting method itself. Therefore, we simply assumed a linear relationship, as shown in Eq.(1), from the bay mouth to the inner bay to roughly estimate the bay-scale tsunami deformation (amplification or reduction). If the bay topography is steep enough, the inundation height can be roughly regarded as the local tsunami height along the shoreline, and it is possible to apply this assumption to ria coasts as well. Figure 14 indicates values of a (denoted the amplification factor hereafter) along the Sanriku coast as estimated by the survey data. This type of empirical fitting was only performed for semi-enclosed bays where Green's law is applicable. The amplification factor a is not directly related to the mean inundation height as shown in Figure 11, but it reflects the general behavior of the tsunami inside the bay. The values of a are confined to ± 0.2 around southern Sanriku (38.4-39.0°N), and they become larger in two bays around 39.0°N. Negative values of a are distributed along the northern part of Sanriku, except for Yamada Bay. Therefore, local amplification only occurred in a few bays along the Sanriku coast.

Contrarily, the tsunami maintained a constant height from the bay mouth to the inner bay along the coast from Onagawa to Ofunato (38.4-39.0°N), and the height was amplified from Okirai to Yoshihama Bays in the middle of the Sanriku coast. There are several reasons why the amplification factors are different for each bay: bay bathymetry, tsunami direction, and offshore barriers are some reasons. For example, the local amplification was severe in Okirai and Ryori Bays, but not as strong as in Kamaishi and Miyako Bays. As discussed, Kamaishi Bay had a tsunami barrier, and it reduced tsunami height in the inner bay. And Miyako Bay opens in the northeast direction, which is different from the main direction of the tsunami.

Further regional analysis in detail is necessary to understand the local behavior of this tsunami which can be seen the other manuscripts in this special issue.

5. Conclusion

This is a summary of the nationwide, post-event survey results for the 2011 Tohoku Earthquake Tsunami in Japan. This tsunami was the first case where modern, well-developed tsunami countermeasures faced such an extreme event. One of the most important issues in natural science, engineering, and social science for the global community is to improve tsunami disaster countermeasures based on what can be learned from this catastrophic event. The high-quality, high-density survey dataset collected by about 300 researchers since March 11, 2011, is summarized, and it provides information on various aspects of tsunami behavior for different geometries and conditions.

The major findings from the survey analysis can be summarized as follows. First, tsunami inundation heights were observed along a 2,000 km stretch of the Japanese coast from Hokkaido to Kyushu; high-quality, high-density tsunami inundation heights and run-up heights were measured. Second, the affected area of this event was several times larger than for the Meiji Sanriku Tsunami of 1896. Maximum run-up heights greater than 10 m are distributed along 530 km of coast and maximum run-up heights greater than 20 m are distributed along 200 km of coast, measured directly. Clearly defined regional or bay-scale tsunami amplification or attenuation was observed, and whether amplification or attenuation occurred depends on the bathymetry and relation to the epicenter. The mean inundation height in southern Sanriku is 10-15 meters and there are several peaks along the coast from the northern to middle part of Sanriku. Sanriku was catastrophically impacted by the tsunami; this was caused by both undisturbed tsunami propagation and amplification inside the coastal bays from southern to mid-Sanriku (38.4-39.5°N). However, the incident tsunami height was large along some parts of the northern Sanriku coastline, in the Taro and Noda areas, although the tsunami decayed inside the bays Ogasawara et al. [2012].

In addition, the survey results provide only the maximum water levels. Dynamic information about the tsunami such as velocity [*e.g.*, Fritz et al., 2004] or the time course of the inundation process are required to understand this event in detail. Video and other recorded data will be helpful to estimate the necessary dynamic information. Discussions are now underway about combining survey measurement data, aerial data, and satellite data. Analyses employing these multiple types of data will be important to understand this event and necessary to validate different types of numerical models [Dunbar et al., 2008] and fragility functions [*e.g.* Suppasri et al., 2012]. Notably, local inundation heights and run-up heights differed between neighboring locations. Macro roughness such as sea walls, as well as complex shading and diffraction by structures, may play important roles behind local tsunami behavior and future planing against tsunamis.

Our preliminary analysis indicates that hard structural protection may have resulted in lower overall inundation heights. However, the effectiveness of different protection schemes and evacuation strategies for the quantitative reduction of damages will require detailed analysis once the survey datasets are combined and numerical hindcasts are performed. Detailed data from surveys and from accurate modeling of the tsunami will help with the restoration of the Tohoku area, and they will also be useful for other coastal regions of high tsunami-risk countries around the world. The data are freely available through the survey group's web site (http://www.coastal.jp/tsunami2011/).

Acknowledgments

On behalf of the tsunami joint survey group, the authors, NM and TT, have summarized this manuscript as secretariat of the survey group. This study was made possible by the work of all the surveyors and participating agencies as shown in the appendix. We gratefully acknowledge their individual and sincere contributions to the survey. The authors appreciate Drs. Daniel Cox, of Oregon State University, Tomohiro Yasuda, of Disaster Prevention Research Institute, Kyoto University and Hideaki Yanagisawa, of Tokyo Electric Power Services Co., Ltd. for their suggestions to summarize this manuscript. This study is dedicated to all who have been affected by the earthquake in Japan on March 11, 2011.

Appendix A. Appendix: Member of Joint Survey Group

Shun-etsu Hamaura, Kazuya Miyakawa, Katsuhiko Tanabe, Keisuke Tanaka, Mitsuyuki Tanaka, Tsukasa Watanabe (Aomori Local Meteorological Ob-servatory), Hideo Matsutomi, Kazunori Naoe, Takuya Noumi, Eriko Yamaguchi (Akita University), Shoichi Ando, Yushiro Fujii, Toshihide Kashima, Yasuo Okuda, Bun'ichiro Shibazaki (Building Research Institute), Tsutomu Sakakiyama, Masafumi Matsuyama, Takumi Yoshii (Central Research Institute of Electric Power Industry), Kazuhisa Goto (Chiba Institute of Technology), Takashi Aida, Yuuji Kurata, Mabumi Miyazaki, Katuya Shutou, Jun Suzuki, Hikari Takeuchi (Choshi Local Meteorological Observatory), Takayuki Nakamura (Ehime University), Osamu Fujiwara, Kyoko Kagohara, Haruo Kimura, Junko Komatsubara, Yukari Miyashita, Yuichi Namegaya, Yuki Sawai, Masanobu Shishikura, Koichiro Tanigawa (Geological Survey of Japan, National Institute of Advanced Industrial Science and Tech-nology), Hermann Fritz (Georgia Institute of Technology), Ken-ichi Uzaki (Gunma University), Mikio Sasaki (Hachinohe Institute of Technology), Masato Minami (Hachinohe National College of Technology), Hitoshi Endou, Masaki Hashimoto, Yutaka Kobashigawa, Masamitsu Kumagai, Masahiro Ietsune, Kazuhiko Nakamura (Hakodate Marine Observatory), Aditya Gusman, Kazuomi Hirakawa, Kei Ioki, Yugo Nakamura, Takafumi Nakayama, Yuichi Nishimura, Purna Putra, Ayumi Saruwatari, Yasunori Watanabe, Tomohito Yamada (Hokkaido University), Yasunori Nabetani, Hisamichi

Nobuoka (Ibaraki University), Takashi Tamada (Idea Co. Ltd.), Yuriko Matsubayashi, Toshinori Ogasawara, Shigeki Sakai (Iwate University), Masao Abe, Yutaka Hayashi, Hideki Iino, Kazuhiro Iwakiri, Kazuhiro Kimura, Kenji Maeda, Masami Okada, Hiroaki Tsushima (Japan Meteorological Agency), Taro Kakinuma, Kei Yamashita (Kagoshima University), Shinya Umeda (Kanazawa University), Takahiro Nakamura, Shuji Seto, Tomoyuki Takahashi, Kurokawa Takahiro, Tetsuya Torayashiki (Kansai University), Gozo Tsujimoto, Kohji Uno (Kobe City College of Technology), Shoichi Yoshioka (Kobe University), Norio Dewa, Tetsuya Hayashi, Mitsuyoshi Kitamura, Shusaku Kuroda, Akihiko Nakahira, Takeshi Nozawa, Kazuya Taniwaki (Kochi Local Meteorological Observatory), Kunio Ohtoshi (Kochi University), Takashi Aoyama, Tatsuo Chiba, Hiroshi Enomoto, Kazunori Hirahara, Shigeki Murai, Hiroshi Narayama, Satoshi Yamanaka, Hitoshi Yamazaki, Satoshi Yoshiiri (Kushiro Local Meteorological Observatory), Ryoukei Azuma, Yasuyuki Baba, Daniel Cox, Kyung-Duck Suh, Eiji Harada, Tetsuya Hiraishi, Hiroyuki Ikari, Hajime Mase, Nobuhito Mori, Kazuya Oki, Shingo Suzuki, Tomohiro Yasuda, Nozomu Yoneyama (Kyoto University), Yukio Oshima, Harutomi Sugaya, Mikio Tanaka (Mito Local Meteorological Observatory), Masashi Fujiwara, Hideaki Suzuki, Tatsuya Suzuki (Morioka Local Meteorological Observatory), Masaki Chinda, Shinsuke Ichikawa, Yasuo Kanamaru, Ryouji Niiyama, Akira Saitou, Hidenori Saitou, Michinori Sasaki, Eikichi Shioya, Toshiharu Shibata, Hiroshi Sugita (Muroran Local Meteorological Observatory), Naoyuki Inukai, Tokuzo Hosoyamada (Nagaoka University of Technology), Tomoya Abe, Kwang-Ho Lee, Koji Kawasaki, Tomoaki Nakamura (Nagoya University), Hirohide Kiri, Kenichi Matsushima, Tetsuo Nakaya, Hajime Tanji (National Agriculture Food Research Organization), Koji Fujima, Yasuko Shigihara, Yoshinori Shigihara, Ryota Tsudaka (National Defense Academy), Takuya Izumiyama, Fuminori Kato, Kentaro Kumagai, Takashi Negi, Kenji Noguchi, Jinkatsu Sugeno, Yoshio Suwa, Shuichi Tsuchiya, Kunihoro Watanabe, Yuji Watanabe (National Institute of Land Infrastructure Management), Noritaka Asakawa, Sugimatsu Koichi, Akiyoshi Nakayama, Kimiyasu Saeki, Sano Tomoaki, Hiroshi Yagi (National Research Institute of Fisheries Engineering), Yuka Nishikawa (National Taiwan University), Daisuke Itou (Obihiro Weather Station), Toru Endo, Tsuyoshi Haraguchi, Takaaki Shigematsu (Osaka City University), Natuski Mizutani (Osaka Sangyo Univeristy), Susumu Araki, Mamoru Arita, Hiroshi Kogi, Daisuke Sakai (Osaka University), Kenzo Kumagai, Kiyohiro Okada, Yousuke Ookubo, Tsuyoshi Nagasawa, Tatsuya Niwa, Shunji Takanishi (Pacific Consultants Co., LTD.), Taro Arikawa, Masayuki Banno, Hiroaki Kashima, Yoshiaki Ku-riyama, Yasuyuki Nakagawa, Jun-ichiro Sakunaka, Masaharu Sato, Katsumi Seki, Ken-ichiro Shimosako, Kojiro Suzuki, Shigeo Takahashi, Daisuke Tatsumi, Takashi Tomita, Makoto Washizaki (Port and Airport Research Institute), Takahiko Hasegawa, Teruo Matsuyama, Mitsuharu Nishimura, Hideki Sato, Hirofumi Takano, Kouji Tobe, Hiroshi Yonekawa (Sapporo District Meteorological Observatory), Takeo Fukuda, Minoru Funakoshi, Satoshi Hagiya, Kazumasa kayano, Tooru Kobayashi, Takashi Masaki, Takashi Sa-

saki, Yuka Yoshida (Sendai District Meteorological Observatory), Masanobu Hasebe (Shimizu Corporation), Kenji Harada (Shizuoka University), Atsusi Furuta, Kazunori Ito, Yukinobu Oda, Yuriko Takayama, Kanako Yokota (Taisei Corporation), Jiang Jing-Cai, Hitoshi Murakami, Yasunori Mutoh, Susumu Nakano, Kenichi Nishiyama, Ryoichi Yamanaka (The University of Tokushima), Yoshihiro Asaoka, Hideomi Gokon, Kentaro Imai, Fumihiko Imamura, Sou Kazama, Shu-nichi Koshimura, Akira Mano, Erick Mas, Abdul Muhari, Shosuke Sato, Daisuke Sugawara, Anawat Suppasri, Hitoshi Tanaka (Tohoku University), Tadashi Aki, Tokihisa Fuji, Masanobu Houdai, Kazuhiro Kageyama, Kazuaki Kawata, Shigeaki Kumano, Kouichi Satou, Shinji Takeda, Haruo Taninaka, Yasuaki Yabuuchi (Tokushima Local Meteorological Observatory), Takuya Nakamura (Tokyo District Meteorological Observatory), Hiroshi Takagi (Tokyo Institute of Technology), Yasuei Masame, Akio Okayasu, Yanzi Piao, Takenori Shimozono, Takumi Suzuki (Tokyo University of Marine Science and Technology), Shin-ichi Aoki (Toyohashi University of Technology), Wataru Funayama, Hitoshi Imai, Takafumi Ishiwaki, Mototaka Itou, Eiji Kajiya, Kunihiro Mashimo, Kaneyoshi Mochiduki, Kazuki Okamoto, Munehiro Okuda, Naoki Ueda, Mitsunobu Sawada (Tsu Local Meteorological Observatory), Mamoru Nakamura (University of the Ryukyus), Vassilis Skanavis, Costas Synolakis (University of Southern California), Tomoya Harada, Takeo Ishibe, Masahiko Isobe, Mohammad Heidarzadeh, Haengyoong Kim, Yukio Koibuchi, Satoshi Kusumoto, Haijiang Liu, Satoko Murotani, Akihito Nishiyama, Satoko Oki, Kenji Satake, Shinji Sato, Megumi Sugimoto, Yoshimitsu Tajima, Tomohiro Takagawa, Jiro Tomari, Yoshinobu Tsuji, Toshihiro Ueno (University of Tokyo), Shigehiro Fujino, Gaku Shoji, Satoshi Takewaka (University of Tsukuba), Kazuaki Hamaoka, Tamotsu Kawata, Yoshio Miki, Harutaka Miyamae, Yuichi Satou, Yoshiaki Tokuda, Masahiro Ueda (Wakayama Local Meteorological Observatory), Nobuaki Koike (Wakayama National College of Technology), Miguel Esteban, Ryo Matsumaru, Takahito Mikami, Koichiro Ohira, Akira Ohatani, Tomoya Shibayama, Hiroshi Takagi (Waseda University), Retno Utami Agung Wiyono, Kimitoshi Hayano, Kazuhiko Hayashi, Jun Sasaki, Takayuki Suzuki (Yokohama National University)

References

Dunbar, P., K. Stroker, V. Brocko, J. Varner, S. McLean, L. Taylor, B. Eakins, K. Carignan, and R. Warnken (2008). Long-term tsunami data archive supports tsunami forecast, warning, research, and mitigation. *Pure and Applied Geophysics 165*(11), 2275–2291.

Fritz, H., J. Borrero, C. Synolakis, and J. Yoo (2004). Indian ocean tsunami flow velocity measurements from survivor videos. *Geophysical Research Letters 33*.

Fujii, Y., K. Satake, S. Sakai, M. Shinohara, and T. Kanazawa (2011). Tsunami source of the 2011 off the pacific coast of tohoku, japan earthquake. *Earth Planets Space, this issue*.

Fujima, K., Y. Shigihara, T. Tomita, K. Honda, H. Nobuoka, M. Hanzawa, H. Fujii,

H. Ohtani, S. Orishimo, M. Tatsumi, et al. (2006). Survey results of the indian ocean tsunami in the maldives. *Coastal Engineering Journal 48*(2), 81–97.

Geospatial Information Authority of Japan (GSI) (2011). Off the pacific coast of tohoku earthquake tsunami fault model.

Gokon, H. and S. Koshimura (2012). Mapping of building damage of the 2011 Tohoku earthquake tsunami in Miyagi prefecture. *Coastal Engineering Journal 54*(1), in press.

Goto, C. and Y. Ogawa (1991). Numerical method of tsunami simulation with the leap-frog scheme.

Intergovernmental Oceanographic Commission; IOC-UNESCO (1998). *Post-tsunami survey field guide* (1st ed.). IOC Manuals and Guides.

Ioualalen, M., J. Asavanant, N. Kaewbanjak, S. Grilli, J. Kirby, and P. Watts (2007). Modeling the 26 december 2004 indian ocean tsunami: Case study of impact in thailand. *Journal of Geophysical Research 112*, C07024.

Kakinuma, T., G. Tsujimoto, T. Yasuda, and T. Tamada (2012). Trace survey results of the 2011 Tohoku earthquake tsunami in the north of Miyagi prefecture and numerical simulation of bidirectional tsunamis in Utatsusaki peninsula. *Coastal Engineering Journal 54*(1), in press.

Karlsson, J., A. Skelton, M. Sandén, M. Ioualalen, N. Kaewbanjak, N. Pophet, J. Asavanant, and A. von Matern (2009). Reconstructions of the coastal impact of the 2004 indian ocean tsunami in the khao lak area, thailand. *Journal of Geophysical Research 114*(C10), C10023.

Koketsu, K., Y. Yokota, N. Nishimura, Y. Yagi, S. Miyazaki, K. Satake, Y. Fujii, H. Miyake, S. Sakai, Y. Yamanaka, et al. (2011). A unified source model for the 2011 tohoku earthquake. *Earth and Planetary Science Letters 310*(3), 480–487.

Kumar, B., R. Kumar, S. Dube, T. Murty, A. Gangopadhyay, A. Chaudhuri, and A. Rao (2006). Tsunami travel time computation and skill assessment for the 26 december 2004 event in the indian ocean. *Coastal Engineering Journal 48*(2), 147.

Largest Earthquakes in the World Since 1900 (2011).

Lay, T., C. Ammon, H. Kanamori, L. Xue, and M. Kim (2011). Possible large near-trench slip during the 2011 mw 9.0 off the pacific coast of tohoku earthquake. *Earth Planets Space 63*(7), 687–692.

Lay, T., Y. Yamazaki, C. Ammon, K. Cheung, and H. Kanamori (2011). The 2011 mw 9.0 off the pacific coast of tohoku earthquake: Comparison of deep-water tsunami signals with finite-fault rupture model predictions. *Earth Planets Space 63*(7), 797–801.

Liu, P., P. Lynett, H. Fernando, B. Jaffe, H. Fritz, B. Higman, R. Morton, J. Goff, and C. Synolakis (2005). Observations by the international tsunami survey team in sri lanka. *Science 308*(5728), 1595.

Matsutomi, H., T. Sakakiyama, S. Nugroho, and M. Matsuyama (2006). Aspects of inundated flow due to the 2004 indian ocean tsunami. *Coastal Engineering*

Journal 48(2), 167–195.

Michelini, A., V. Lauciani, G. Selvaggi, A. Lomax, et al. (2010). The 2010 chile earthquake: Rapid assessments of tsunami. *EOS*.

Mikami, T., T. Shibayama, M. Esteban, and R. Matsumaru (2012). Field survey of the 2011 Tohoku earthquake and tsunami in Miyagi and Fukushima prefectures. *Coastal Engineering Journal 54*(1), in press.

Mori, N., T. Takahashi, T. Yasuda, and H. Yanagisawa (2011). Survey of 2011 tohoku earthquake tsunami inundation and run-up. *Geophysical Research Letters 38*(1), L00G14.

Ogasawara, T., Y. Matsubayashi, S. Sakai, and T. Yasuda (2012). Characteristics on tsunami disaster of northern Iwate coast of the 2011 Tohoku earthquake tsunami. *Coastal Engineering Journal 54*(1), in press.

Sasaki, J., K. Ito, T. Suzuki, R. U. A. Wiyono, Y. Oda, Y. Takayama, K. Yokota, A. Furuta, and H. Takagi (2012). Behavior of the 2011 Tohoku earthquake tsunami and resultant damage in Tokyo bay. *Coastal Engineering Journal 54*(1), in press.

Shimozono, T., S. Sato, A. Okayasu, Y. Tajima, H. M. Fritz, H. Liu, and T. Takagawa (2012). Propagation and inundation characteristics of the 2011 Tohoku tsunami on the central sanriku coast. *Coastal Engineering Journal 54*(1), in press.

Suppasri, A., S. Koshimura, K. Imai, E. Mas, H. Gokon, A. Muhari, and F. Imamura (2012). Field survey and damage characteristic of the 2011 east Japan tsunami in Miyagi prefecture. *Coastal Engineering Journal 54*(1), in press.

Suppasri, A., E. Mas, S. Koshimura, K. Imai, K. Harada, and F. Imamura (2012). Developing tsunami fragility curves from the surveyed data of the 2011 east Japan tsunami in Sendai and Ishinomaki plains. *Coastal Engineering Journal 54*(1), in press.

Tanaka, H., N. X. T. andRyutaro Hirao, M. Umeda, E. Pradjoko, A. Mano, and K. Udo (2012). Coastal and estuarine morphology changes induced by the 2011 great east Japan earthquake tsunami. *Coastal Engineering Journal 54*(1), in press.

The 2011 Tohoku Earthquake Tsunami Joint Survey Group (2011). Nationwide field survey of the 2011 off the pacific coast of tohoku earthquake tsunami. *Journal of Japan Society of Civil Engineers, Series B 67*(1), 63–66.

Tomita, T., F. Imamura, T. Arikawa, T. Yasuda, and Y. Kawata (2006). Damage caused by the 2004 indian ocean tsunami on the southwestern coast of sri lanka. *Coastal Engineering Journal 48*(2), 99–116.

Udo, K., D. Sugawara, H. Tanaka, K. Imai, and A. Mano (2012). Impact of the 2011 Tohoku earthquake and tsunami on beach morphology along the northern Sendai coast. *Coastal Engineering Journal 54*(1), in press.

Watanabe, Y., Y. Mitobe, A. Saruwatari, T. Yamada, and Y. Niida (2012). Evolution of the 2011 Tohoku earthquake tsunami on the Pacific coast of Hokkaido.

Coastal Engineering Journal 54(1), in press.

Yamamoto, Y., H. Takanashi, S. Hettiarachchi, and S. Samarawickrama (2006). Verification of the destruction mechanism of structures in sri lanka and thailand due to the indian ocean tsunami. *Coastal Engineering Journal 48*(2), 117–145.

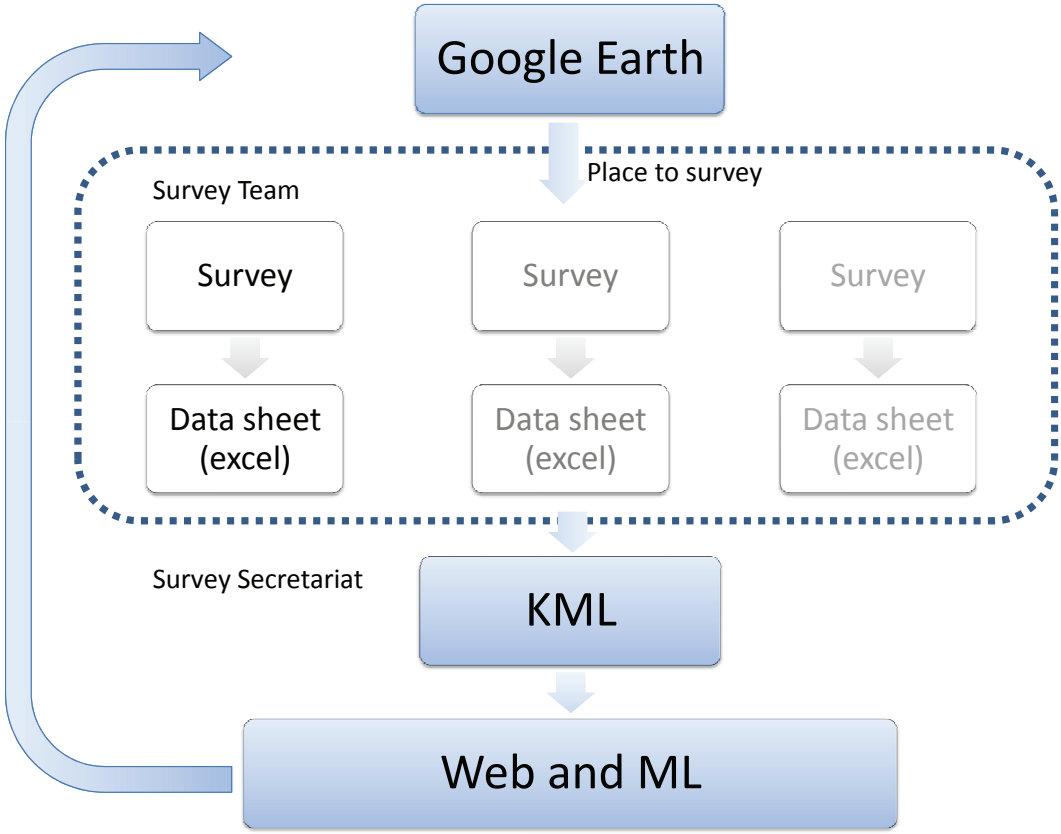

Fig. 1. Flowchart for collecting and distributing survey data

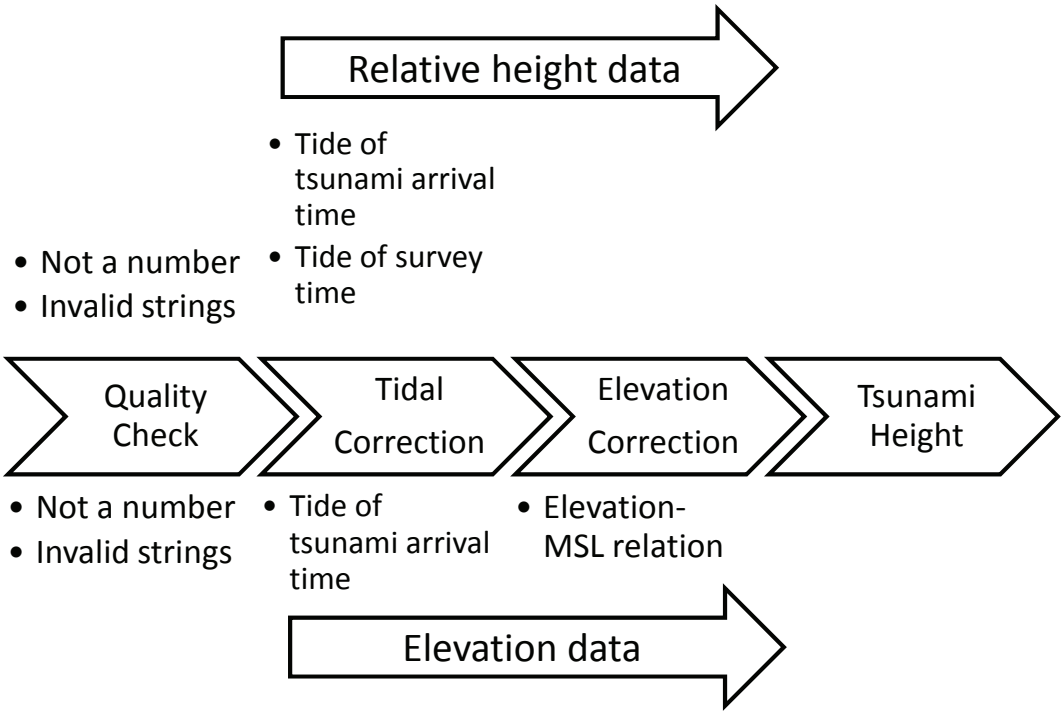

Fig. 2. Data process for tidal correction

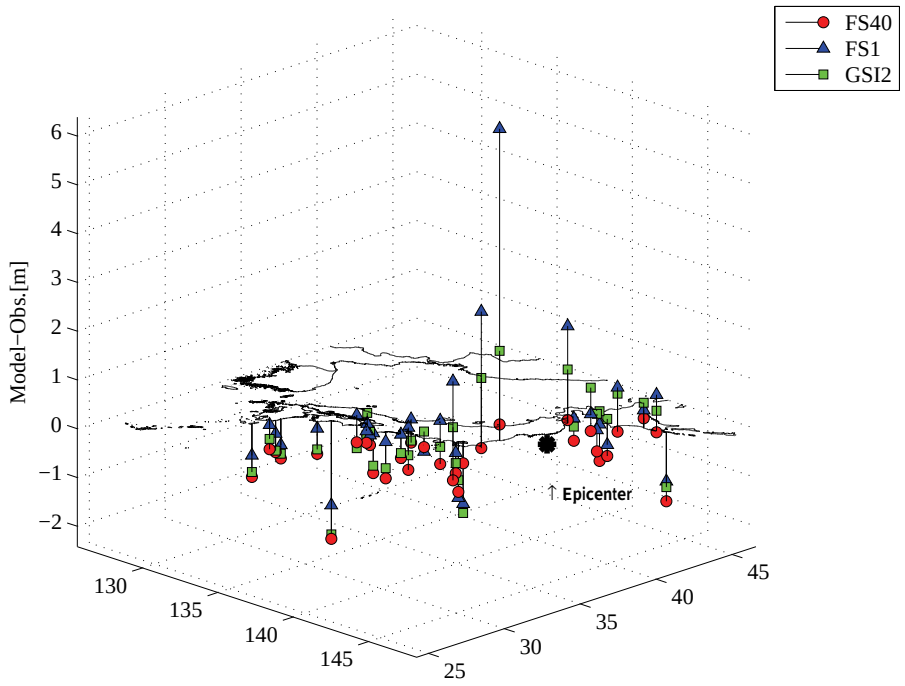

(a) Height

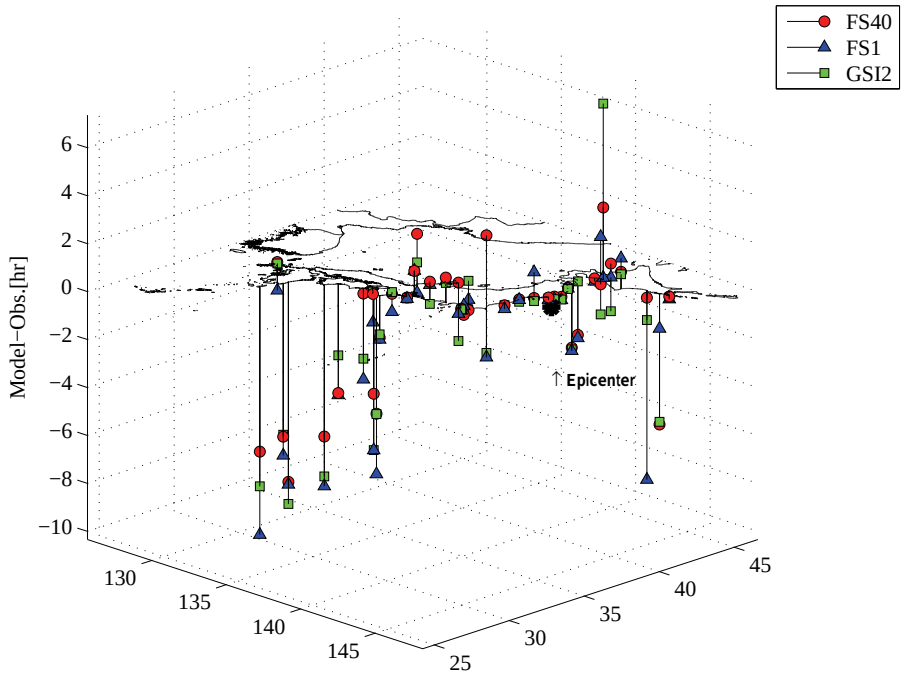

(b) Arrival time

Fig. 3. Maximum computed tsunami height and arrival time for different offshore tsunami sources (•: Fuji 40-subfaults model version 4.6, △: Fuji 1-fault model, □: GSI 2-faults model, *: epicenter)

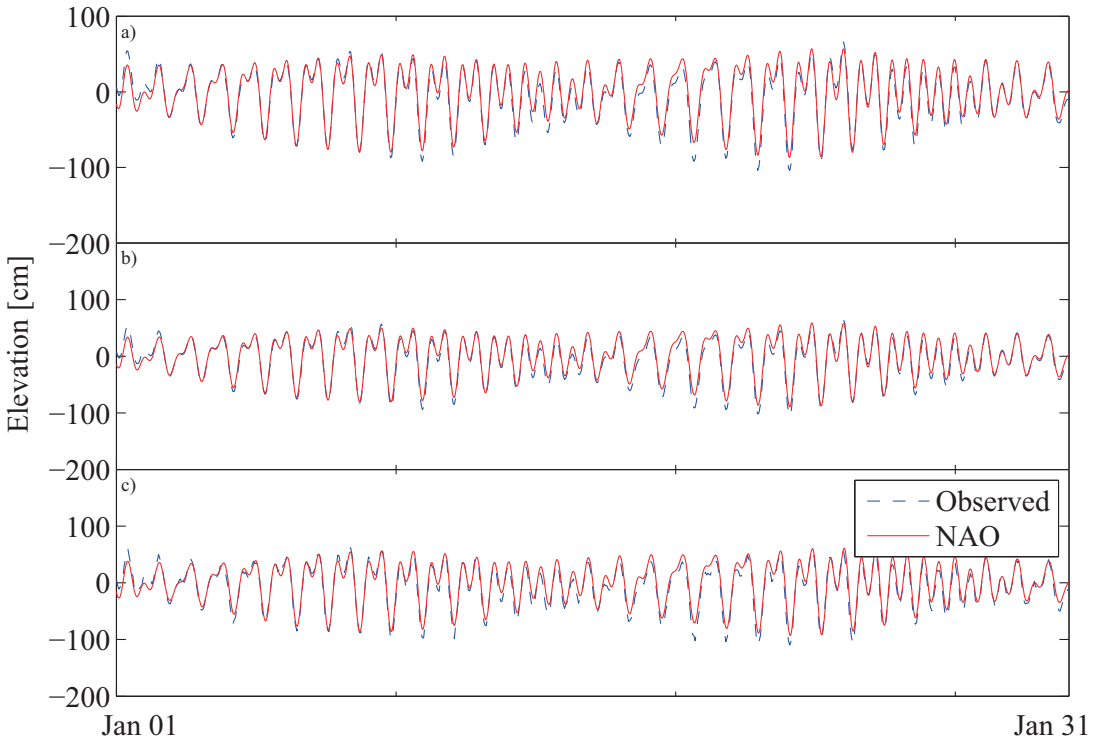

Fig. 4. Comparison of tidal elevation between database and observed data (top: Hachinohe, middle: Ofunato, bottom: Sendai; solid line: tidal database, dashed line: tide gauge)

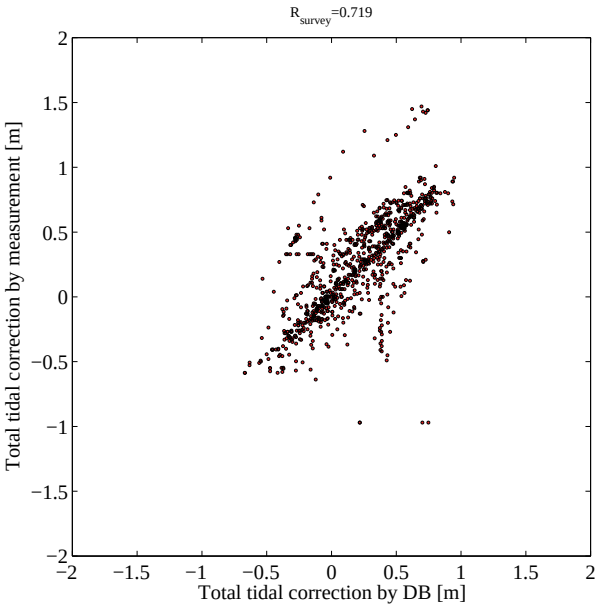

(a) Relation of estimated tidal correction between database and tide gauge

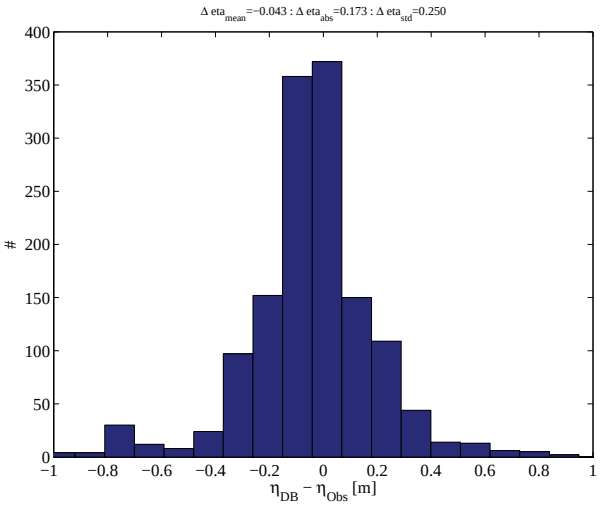

(b) Histogram of relative error

Fig. 5. Validation of tidal correction

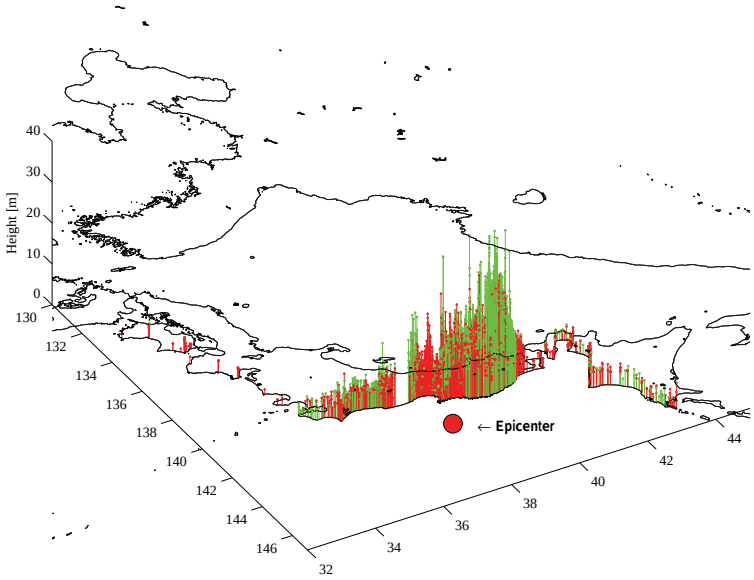

Fig. 6. Measured inundation and run-up heights around the Pacific coast of Japan (Darker and lighter colored bars indicate inundation height and run-up height, respectively.)

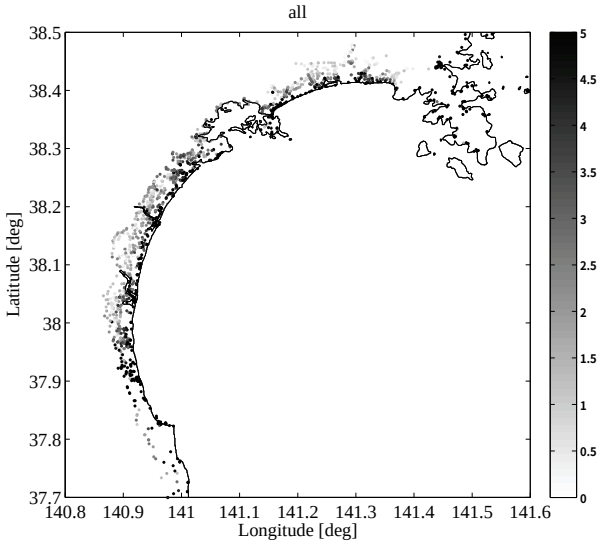

Fig. 7. Measured inundation and run-up heights around the Sendai plain

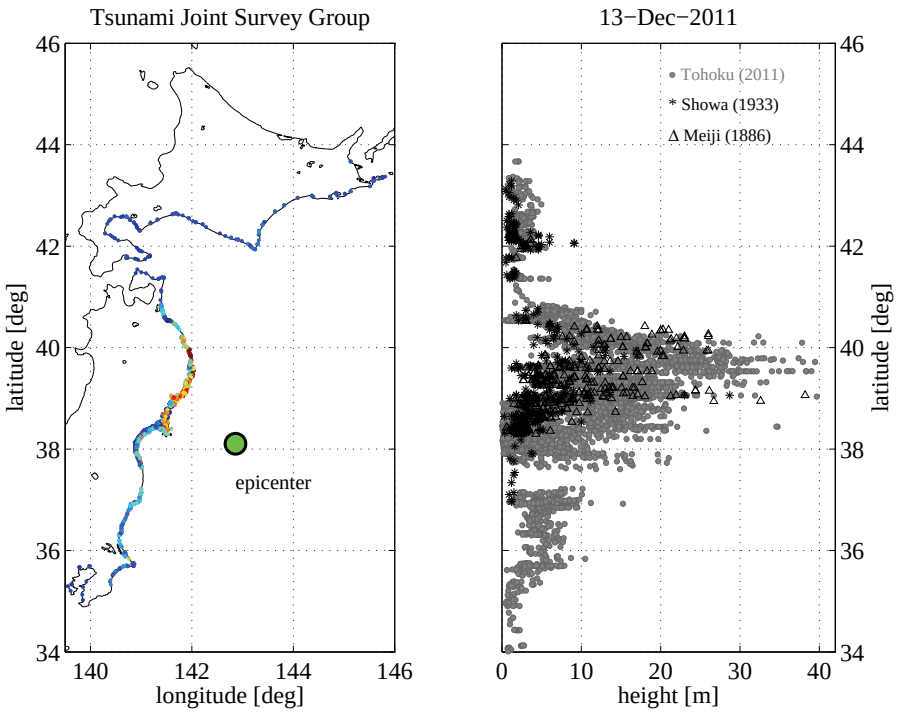

Fig. 8. Measured tsunami heights versus latitude, including previous tsunami records (•: This event (inundation and run-up heights), ♢: Showa Sanriku tsunami, △: Meiji Sanriku tsunami)

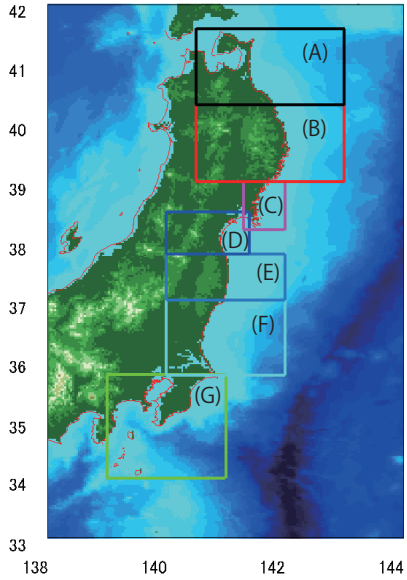

(a) Area of analysis

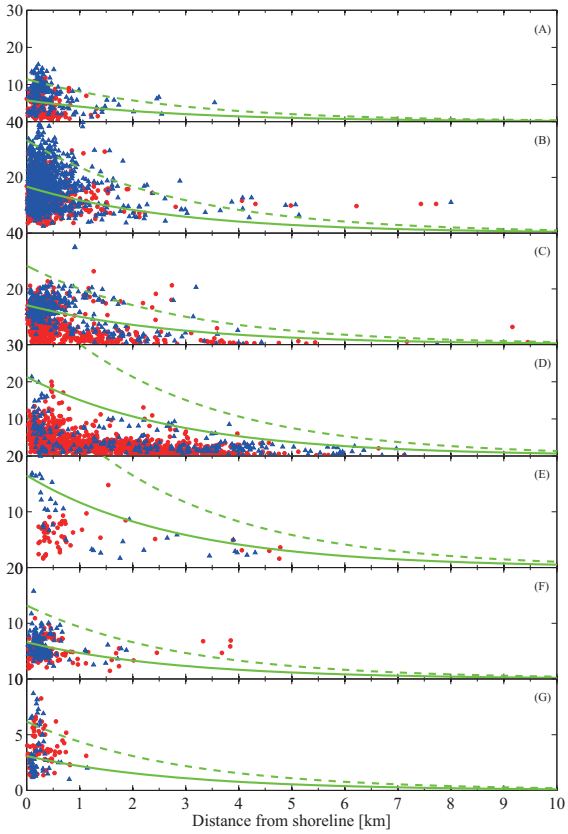

(b) Inundation distance from coast line

Fig. 9. Regional analysis of tsunami inundation height (unit:m) and distance (unit: km; •: inundation height, △: run-up height, lines: empirical curve)

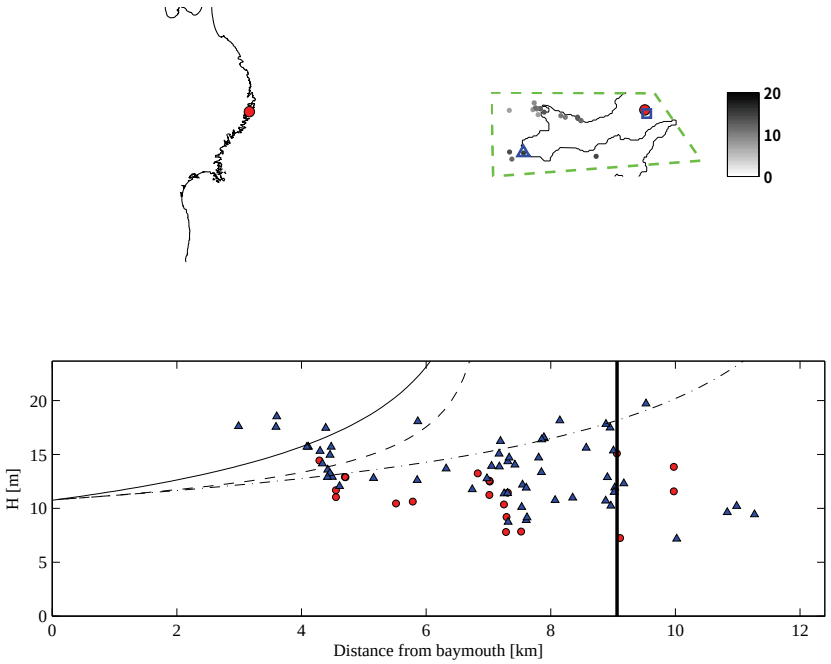

(a) Otsuchi Bay in Iwate Prefecture

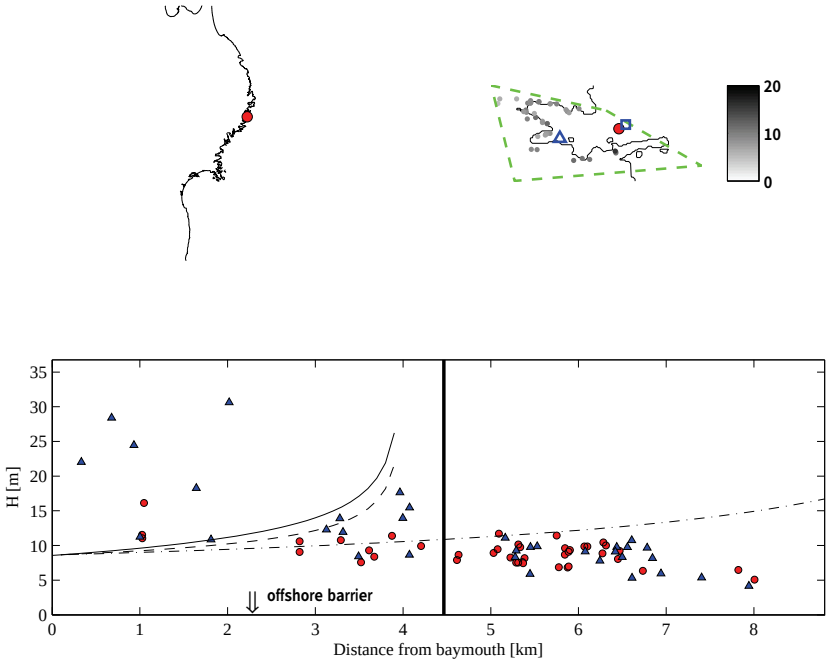

(b) Kamaishi Bay in Iwate Prefecture

Fig. 10. Example of bay scale analysis of inundation and run-up heights (region (B) in Figure 9) (top left panel: bay location; top right panel: □: location of bay mouth, △: location of shoreline ; bottom panel: •: inundation height, △: run-up height, lines: Green's law, solid vertical line: shoreline)

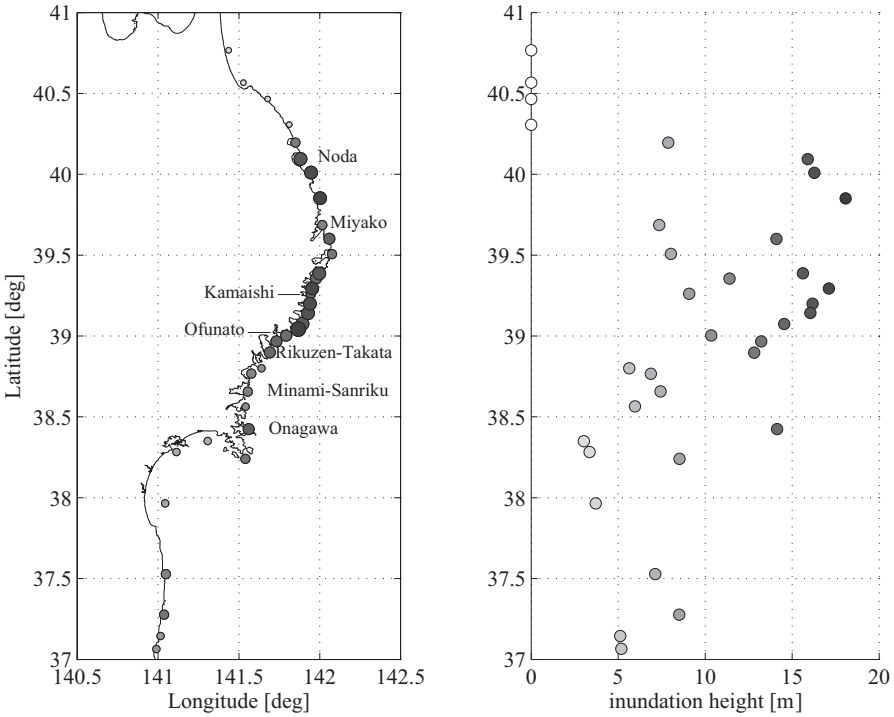

Fig. 11. Bay-scale averaged inundation height along Tohoku coast (unit:m)

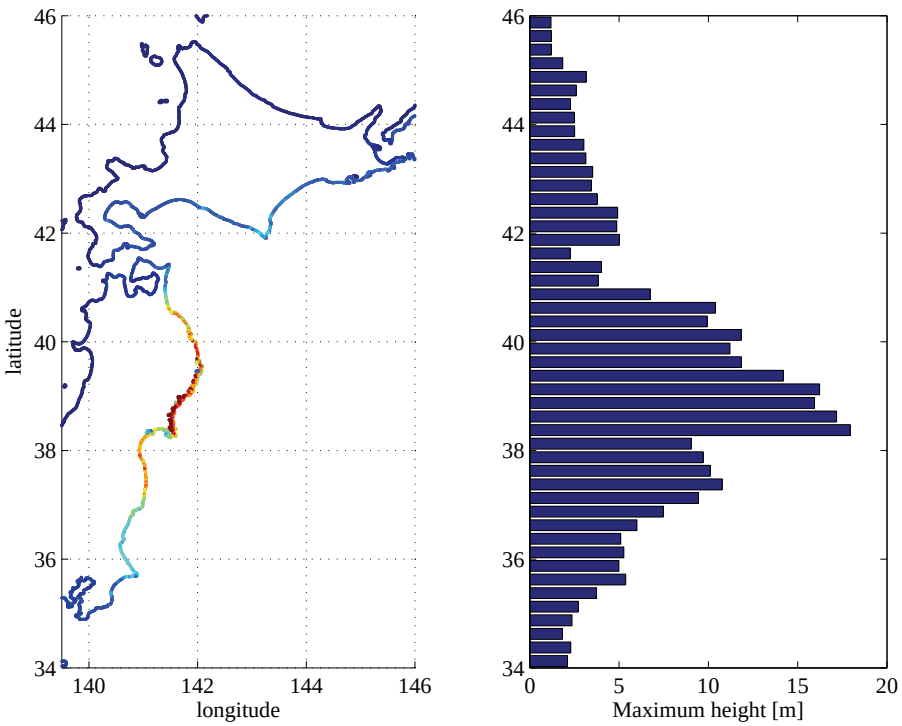

Fig. 12. Simulated maximum tsunami height along Sanriku coastline (initial condition: FS40v46, unit:m)

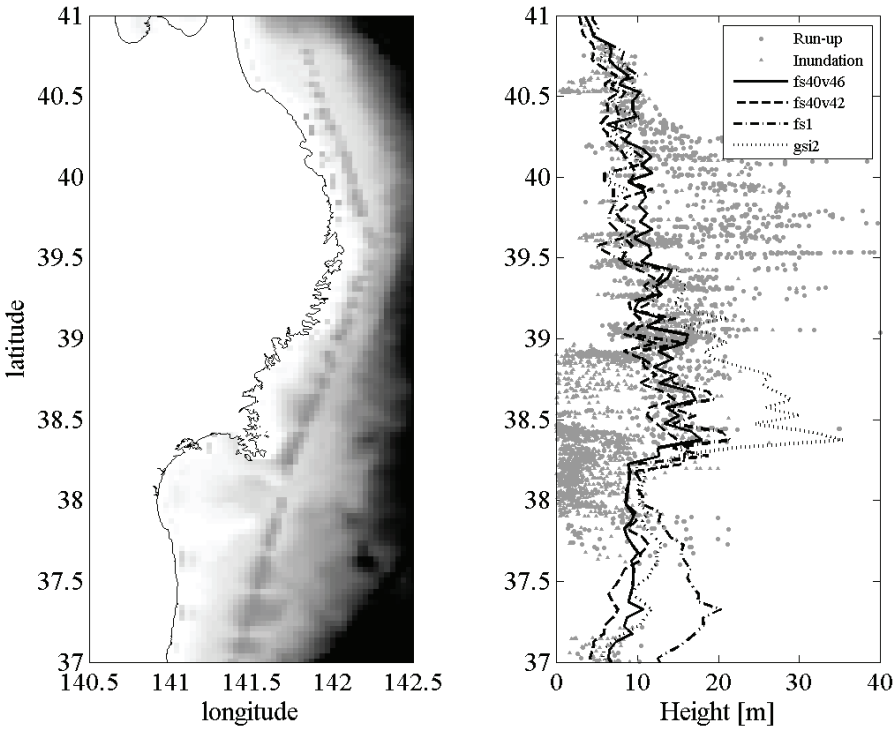

Fig. 13. Comparison of simulated maximum tsunami height with survey data along Sanriku coastline (lines: numerical results by different initial conditions of FS40v42, FS40v46, FS1 and GSI2; marks: survey data) (unit:m)

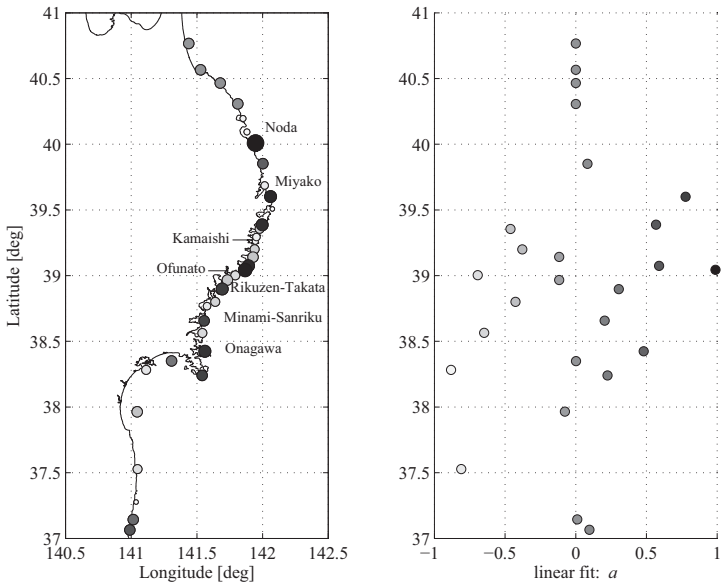

Fig. 14. Distribution of estimated amplification factor a (m/km) of inundation/run-up heights from the bay mouth